

N73 15027

**NASA TECHNICAL
MEMORANDUM**

NASA TM X- 68172

NASA TM X- 68172

**CASE FILE
COPY**

**EXTERNALLY BLOWN FLAP TRAILING EDGE NOISE REDUCTION
BY SLOT BLOWING--A PRELIMINARY STUDY**

by D. J. McKinzie, Jr. and R. J. Burns
Lewis Research Center
Cleveland, Ohio

TECHNICAL PAPER proposed for presentation at
Eleventh Aerospace Sciences Meeting and Technical Display
sponsored by the American Institute of Aeronautics and Astronautics
Washington, D.C., January 10-12, 1973

EXTERNALLY BLOWN FLAP TRAILING EDGE NOISE REDUCTION BY SLOT BLOWING--
A PRELIMINARY STUDY

D. J. McKinzie, Jr.* and R. J. Burns**

Lewis Research Center
National Aeronautics and Space Administration
Cleveland, Ohio

Abstract

Short takeoff and landing (STOL) aircraft using externally blown flaps (EBF) for lift augmentation develop considerable jet-flap interaction noise. A proposed method to reduce the EBF trailing edge noise is to locate a slot near the trailing edge of a flap through which low velocity secondary air is blown. Limited OASPL noise data were obtained from the interaction of the jet exhaust from a 5.08 cm diameter convergent nozzle with the trailing edge of a plate, and are presented for five slot configurations located near or at the trailing edge of the plate. Also presented are some significant jet trailing edge interaction data using a mixer nozzle with one of the slot configurations.

Introduction

The externally blown flap (EBF) being considered as a lift augmentation device in a short takeoff and landing (STOL) aircraft generates considerable jet-flap interaction noise.⁽¹⁻⁴⁾ The flap noise results primarily from the interaction of the fan-jet engine exhaust with the leading and trailing edges of the flaps^(5,6) between their fully retracted position and their landing position. The edges are believed to act as approximately equal noise sources,⁽⁴⁾ therefore, they must each be treated to reduce the noise.

In Ref. 7, Benjamin Pinkel and Terry D. Scharton of Bolt, Beranek and Newman described a method of reducing the EBF trailing edge noise. They proposed to locate a slot near the trailing edge of a flap through which secondary air is blown at low velocity. They performed small scale tests using a 1.59 cm diameter circular nozzle and flat plates to simulate the flap trailing edge surfaces. However, their tests were run at only one nozzle and plate orientation simulating the geometry of the proposed STOL aircraft landing configuration.⁽⁴⁾ Specifically, in Ref. 7, the axial distance between the nozzle exit and plate was set equal to four nozzle diameters, while Ref. 4 indicates that this distance may vary between approximately 4 and 7 nozzle diameters. This difference is important because within it the growth and decay of the large scale ring vortices and jet turbulence occur⁽⁸⁾ which are believed to be sources of jet noise.

Though Pinkel and Scharton⁽⁷⁾ did not offer an explanation of the mechanism by which trailing edge blowing reduces noise, a possible explanation of how the noise is generated at the trailing edge of a plate is offered by the following considerations. Reference 9 presents studies of a simple subsonic jet which show a very strong correlation between the far field noise and the magnitude and frequency

of the oscillating component of the static pressure in a free jet about five diameters from the nozzle exit. This oscillating static pressure is believed to be produced by large scale eddies in the jet generated by the mixing of the jet with the ambient air. Pinkel and Scharton⁽⁷⁾ suggest that the eddies developed in the jet exhaust stream impinge on a flat plate and move along the plate to the trailing edge where they generate noise that can be approximately 20 dB greater than the noise of the free jet. Experimental results of Ref. 7 show that this large trailing edge noise level may be reduced by from 4 to 6 dB at jet Mach numbers of 0.9 and 0.5, respectively, by using trailing edge blowing.

This paper presents experimental noise data obtained from the interaction of the cold jet exhaust from a 5.08 cm diameter convergent nozzle with the trailing edge of a flat plate. The test geometry simulates approximately the jet exhaust orientation to the trailing edge of the second flap of the EBF system discussed in Ref. 2 and shown in Fig. 1. A small amount of data were also obtained using a 6-tube mixer nozzle similar to one studied in Ref. 10. The flat plate used in these studies represents a simplification of a blown-flap configuration in which the flap trailing edge surfaces are replaced with flat plates. The tests were conducted to study the qualitative noise reductions resulting from the interaction of air blowing through a slot near or at the trailing edge of a flat plate with the jet exhaust directed at the plate in the vicinity of its trailing edge. They were made at a larger scale than that of Ref. 7 and over a more broad range of test and geometrical configuration variables. The noise reductions were determined by comparing noise data obtained with the slot open and slot covered.

Apparatus and Procedure

Facility

The noise tests were conducted out-of-doors within the 7 x 15 m courtyard of a subsonic wind tunnel at the Lewis Research Center. The courtyard permitted noise data to be taken with both a 5.08 cm diameter D convergent nozzle and a 6-tube mixer nozzle. The flow system for the nozzles will hereafter be referred to as the primary system. The nozzles axes were located in the horizontal plane approximately 1.2 m above a gravel covered ground surface. A flat plate 76 cm long by 43 cm wide was oriented to either nozzle so that its impact surface was in the vertical plane and could be rotated about a vertical axis. The plate had two degrees of freedom in the horizontal plane and was positioned so that the jet exhaust from either nozzle could be directed at it in the vicinity of

*Aerospace Engineer, NASA-Lewis Research Center, AIAA Member.

**Aerospace Engineer, NASA-Lewis Research Center.

its trailing edge. The plate was mounted on a 78 cm long plenum chamber which supplied air to the trailing edge slot configurations tested (see fig. 2). The flow system for the plenum chamber will hereafter be referred to as the secondary system.

Cold dry air at $292 \text{ K} \pm 14 \text{ K}$ and 850 kN/m^2 was supplied to the primary and secondary flow systems. Perforated plates and a muffler were located in each system to remove valve noise from the measured noise. In addition, a bundle of tubes was placed in the supply line (15.2 cm diameter) of the primary system to straighten the air flow before it reached the entrance to the nozzle. These devices were located well upstream of the nozzle. To aid in distributing the air in the plenum chamber of the secondary system a perforated 5.3 cm diameter tube was installed along the length of the plenum and was fed at both ends by a 5.1 cm diameter inlet line. The mass flow rates through the primary and secondary systems were measured by flat plate orifices installed in separate orifice runs according to ASME specifications.

The overall sound pressure level (OASPL) data were read out on the 20 kc scale of a portable General Radio sound-level meter in decibels referenced to $2 \times 10^{-5} \text{ N/m}^2$. A crystal microphone with wind screen was used. Spectral noise data (SPL) were obtained using a 1.27 cm diameter condenser microphone with wind screen. The noise data were recorded on a FM tape recorder and digitized by a four second time averaged one-third octave band spectrum analyzer. The analyzer determined sound pressure level spectra in decibels referenced to $2 \times 10^{-5} \text{ N/m}^2$.

Test Conditions

OASPL noise data were taken along a 120 degree horizontal arc of a 3.05 m radius circle centered on the exit of the nozzle. The noise data were taken at angles θ on the microphone circle of 90, 105, 120, 135, 158, 180, 190, 200, and 210 degrees measured from the up-stream axis of either the convergent or mixer nozzle. The condenser microphone was located at either the 93 or 102 degree position on the microphone circle. All of the noise data were taken at jet Mach numbers M_p of approximately 0.4, 0.5, 0.7, and 0.9.

Test Configurations

Five slot configurations were tested and are shown in Figs. 3(a) to (e). Slot configurations 1, 2, and 3 (figs. 3(a), (b), and (c)) had the slot located in the surface of the flat plate near its trailing edge. These configurations were tested to determine the noise reduction produced as a function of, (1) their differences in dimensionless throat height y/D , and (2) changes made in the lip length x measured between their trailing edge and the downstream edge of the slot. Slot configuration 4 (fig. 3(d)) represents a limit in which the lip length equals zero. Configuration 5 (fig. 3(e)) has a slot located at a step near the trailing edge of a plate. The step length was varied to show the effect of the semibounded slot flow on the noise reduction. The spanwise length of the slot configurations was set at approximately 15, 20, and 76 cm during portions of the tests. The mixer nozzle was designed using Ref. 10 to produce a decay in velocity, at the plate, to 45 percent of the peak nozzle

exit velocity, and to have the same effective flow area as the convergent nozzle. The six tubes had an inside diameter of 2.21 cm, were equally spaced on a 9.5 cm diameter circle of a 15.25 cm pipe flange, and were 6.2 cm long. The mixer nozzle was run only with the step slot configuration.

In addition to the configuration variables, two additional dimensionless position variables were studied which describe the location of the plate in relation to the jet and nozzle exit, see Fig. 2. The first of these z/D represents the dimensionless axial separation distance between the nozzle exit and the surface of the plate. Three axial test positions were chosen for investigation. Two of the test positions, $z/D = 7$ ($\gamma = 60^\circ$) and 9 ($\gamma = 20^\circ$), correspond to the EBF aircraft landing and takeoff configuration⁽²⁾; additional data were taken at $z/D = 4$ ($\gamma = 25^\circ$). γ represents the acute angle between the plane of the plate and the jet nozzle axis. The second position variable a/D (fig. 2) represents the lateral distance, in the plane of the plate, between its trailing edge and the nozzle axis. It varied between the limits of $a/D = -1$ and $a/D = 4$.

Table I presents a summary of the five slot configurations tested and their subvariations. The Mach number M_{slot} of the flow through the slot configurations, of table I, was held constant during each test. However, throughout the tests it was varied between approximately 0.25 and 0.6, depending on the configuration and the jet Mach number, M_p .

To determine the value of the noise reduction produced by the slot configurations (open slot data), data were also taken with the slot covered, hereafter referred to as a flat plate configuration. This was done by covering the slot with shim stock and masking tape. Thus, the difference between the OASPL noise levels, in decibels, produced by a flat plate configuration and a slot configuration represents a noise reduction, which is designated here with a positive sign. Thus,

OASPL Noise Reduction =

$$\text{OASPL}_{\text{flat plate}} - \text{OASPL}_{\text{slot open}}$$

Results and Discussion

The test results are presented in three forms: first, OASPL noise reduction data are presented in plotted and tabular form as a function of nozzle exit Mach number, M_p ; second, SPL data are presented as a function of the 1/3 octave band center frequency f ; and third, some flat plate data, obtained from the convergent and mixer nozzles, are presented for comparison as a function of the angular location around the microphone circle, θ . Test data from the open slot configurations are compared with data obtained using a flat plate configuration.

OASPL Noise Reduction Data

Figures 4 and 5 show regions bounded by the largest and smallest OASPL noise reductions obtained while varying M_p for $a/D = 0$, and 1. In each *some of the* regions a labeled curve is shown which represents the noise reduction obtained at $\theta = 90$ degrees. The upper and lower limits of the regions labeled; range of data $\theta = 90$ to 135 degrees, represent an envelope indicating the largest and smallest noise

reduction, respectively, produced between the angles of 90 and 135 degrees of the microphone circle. This range of angles contains the most meaningful data for flyover interpretation.

Figure 4 presents the noise reduction data for slot configurations 1, 2, and 3 located at $z/D = 4$, $\gamma = 25$ degrees, and having a slot length of either 20 or 76 cm. With the trailing edge located at $a/D = 1$ (fig. 4(a)), configuration 1 produced the largest noise reduction (up to 4 dB) at $M_p = 0.4$, 0.5, and 0.7, while configuration 2 produced the largest noise reduction (up to 2.5 dB) at $M_p = 0.9$. With the trailing edge located at $a/D = 0$ (fig. 4(b)), slot configuration 1 produced noise at $M_p = 0.5$ and above, while configuration 3 (fig. 4(f)) produced a noise reduction at $M_p = 0.4$, 0.5, and 0.7, but not at 0.9; no data are presented for configuration 2.

Figure 4 also presents data obtained from slot configurations 1 and 2 (figs. 4(a) and (d)) having lip lengths, x , of 0.95 and 2.06 cm, which demonstrate the effect of a change in the dimensionless slot throat height, y/D , on the noise reduction. Although their lip lengths are not the same, the lengths measured between plate's trailing edges and the upstream edges of their slots are the same. Thus, the slots are believed similarly placed, since the point at which the air enters the flow field above the surface of the plates, in relation to their trailing edges, is the same. A comparison of the configurations' noise reductions shows that configuration 1, with the larger throat height, produced a larger reduction in the noise. Specifically, the ratio of the throat heights is 2.4 with an average difference of approximately 2 dB in the noise reduction.

With the trailing edge of slot configuration 2 located at $a/D = 1$, a comparison of the data in Figs. 4(c) and (d) show the effect on noise reduction of a change in lip length. The data show that the shorter lip length produced a greater noise reduction, though the relationship is weak. That is, the ratio of the lip lengths is 4.3 with an average difference of 1 dB in noise reduction.

Tables II and III present the OASPL noise reduction data obtained from configurations 1, 2, and 3 at z/D of 7 ($\gamma = 60^\circ$) and 9 ($\gamma = 20^\circ$), respectively. The columns, labeled region of data at $a/D = 1$ and 0, represent the largest and smallest OASPL noise reductions obtained between the angles $\theta = 90$ and 135 degrees of the microphone circle, while varying M_p . The data in table II were obtained with the axial location and angular orientation of the plate corresponding approximately to the EBF landing configuration shown in Fig. 1(b). Slot configuration 2 produced noise reductions of approximately 2 dB which were greater than those of configurations 1 and 3, at $a/D = 1$. The noise reductions produced by configuration 3, however, were more uniform, as shown by the smaller spread in the data. Table III presents the data obtained with the plate oriented to the exit of the nozzle corresponding approximately to the EBF takeoff configuration shown in Fig. 1(a) in which $a/D = 0$. The noise reductions produced by the three configurations are so small that they are all mutually ineffective.

Though the effect on noise reduction of a change in z/D at a constant value of γ and

a/D is of interest these conditions were not met exactly for any of the slot configurations tested. However, Fig. 5 presents data which represent a close approximation, using slot configuration 1. With the trailing edge located at $a/D = 0$, Fig. 5(a), the data obtained at $z/D = 4$ for $\gamma = 25$ degrees and at $z/D = 9$ for $\gamma = 20$ degrees indicate that slot blowing produced approximately a one decibel increase in noise above that produced by the flat plate. However, with the trailing edge at $a/D = 1$, Fig. 5(b), slot blowing resulted in an average decrease in noise of approximately 1 and 1 dB below that produced by the flat plate at $z/D = 4$ and 9, respectively. Thus, slot configuration 1 more effectively reduces noise at $z/D = 4$, $a/D = 1$, and for $\gamma = 25$ degrees.

Figure 6 presents the noise reduction data for slot configurations 4 and 5 located at $z/D = 7$ and $\gamma = 60$ degrees. Data obtained using two different lengths of spanwise slots, 15 and 76 cm, are presented for configuration 4. With the trailing edge located at $a/D = 1$ and a slot length of 15 cm, neither configuration 4 or 5, Figs. 6(a) and (e), respectively, produced noise reductions greater than 2.5 dB. At $a/D = 0.25$, slot configuration 4, Fig. 6(c), produced noise reductions of as much as 4.5 dB for M_p between 0.4 and 0.7 and a slot length of 76 cm. At $a/D = 0$, both configurations, Figs. 6(d) and (f), produced similar noise reductions with a peak of approximately 3.5 dB.

Spectral Data

Figures 7 to 11 present typical SPL noise data as a function of one-third octave band center frequency, f , for slot configurations 2, 4, and 5, at $z/D = 7$ and $\gamma = 60$ degrees, compared with flat plate data. The data presented in Fig. 7 were taken with the microphone located at $\theta = 93$ degrees on the microphone circle, while the data shown in Figs. 8 to 11 were taken with the microphone at $\theta = 102$ degrees.

The data shown in Fig. 7 ($a/D = 1$) indicate that no significant change in the spectral distribution occurred with air blowing through the slot of configuration 2 (open symbols) as compared with the flat plate data (dark symbols).

Figure 8 presents the spectral data for slot configuration 4 ($a/D = 1$) which indicate that a change took place in the spectral distribution in the higher frequency range. Also, noise reductions up to 5.5 dB occurred at frequencies of approximately 5600 Hz. Such reductions may be realizable in a full scale design at several hundred hertz, if scaling permits. Figure 9, ($a/D = 0$) indicates that configuration 4 produced noise reductions in the high frequency range at $M_p = 0.4$ and 0.5. Figure 10 presents results obtained using slot configuration 5 ($a/D = 1$) which indicate noise reductions up to 3.5 dB occurred in the frequency range above 2000 Hz. The SPL data shown in Fig. 11 ($a/D = 0$) indicate that more noise was generated at the higher frequencies for $M_p = 0.4$ and 0.5 than produced by the flat plate. Therefore, slot configuration 4 produces more noise reduction than configuration 5 especially at trailing edge locations of $a/D = 1$ and 0. This difference may be due to the fact that configuration 5 has two trailing edges (fig. 3(e)) over which the jet exhaust must flow, while configuration 4 has one. Thus, the additional trailing

edge of configuration 5 may act as an additional source of high frequency noise.

Peak Spectral Data

In Figs. 7, 8, and 10 (slot configurations 2, 4, and 5, respectively) the peak flat plate spectral data occur at a constant frequency of either 2000 Hz or 2500 Hz for $M_p = 0.4, 0.5, 0.7,$ and 0.9 , with the trailing edge at $a/D = 1$. Thus, the jet exit velocity v would vary inversely with the Strouhal number fD/v computed at these peak frequencies. In contrast, the flat plate spectral data shown in Figs. 9 and 11 (slot configurations 4 and 5, respectively), with the trailing edge at $a/D = 0$, indicate that the peak frequencies occur at an average Strouhal number of 0.34. This result is of interest because experimental data from Ref. 11 indicate that the shearing frequency of the large ring vortices from a convergent nozzle is dependent on a Strouhal number of approximately 0.3. Thus, the difference in Strouhal number dependence at $a/D = 0$ and $a/D = 1$ may be explained by the following considerations. When the trailing edge of a flat plate lies on the axis of a jet exhaust, $a/D = 0$, the noise data presented here indicate that the ring vortices propagating downstream from the nozzles exit and flowing past the trailing edge are influencing the noise produced. Further, as the trailing edge moves across the axis of the jet exhaust to a point one nozzle diameter from it, $a/D = 1$, the data presented here may indicate that the large ring vortices have been replaced as the major noise source.

Mixer Nozzle Data

OASPL noise data were obtained using configuration 5 with a 6-tube mixer nozzle. The exit plane of the mixer nozzle tubes was positioned in the same plane relative to the flat plate and its trailing edge as was the convergent nozzle. With the trailing edge at $a/D_e = 2.3$, noise data were obtained with slot configuration 5 located at $z/D_e = 16.1$, $\gamma = 60$ degrees, and having a slot length of 15 cm. D_e represents the inside diameter of the tubes. The slot had a dimensionless height of $y/D_e = 0.12$ and step length $x = 1.2$ cm. Noise reductions of 0.7 dB were uniformly obtained between $\theta = 90$ and 120 degrees at $M_p = 0.4, 0.5, 0.7,$ and 0.9 . Figure 12 presents flat plate data obtained using the convergent and mixer nozzles, thus providing a comparison between their OASPL noise levels. In the 90 to 120 degree range along the microphone circle, the difference in the OASPL noise data obtained with the convergent and mixer nozzles varied from a maximum of 14.5 dB at $\theta = 90$ degrees and $M_p = 0.9$ to a minimum of 7.5 dB at $\theta = 90$ degrees and $M_p = 0.7$. Only the OASPL noise data obtained at nozzle Mach numbers, M_p , of 0.7 and 0.9 are presented because the mixer nozzle noise data obtained at Mach numbers of 0.4 and 0.5 were affected by the 75 dB background noise level existent in the courtyard of the test facility.

Reference 12 presents OASPL noise data obtained from the interaction of a large scale 7-lobe mixer nozzle (equivalent to a 33 cm diameter convergent nozzle) and externally blown flaps positioned in the 30-60 degree landing configuration. The test results are compared to the scaled noise data obtained using a convergent nozzle positioned in the same relative way to the 30-60 degree flaps. The comparison indicates that the noise level is

about 6 dB uniformly lower with the mixer nozzle blowing on the flaps than with a convergent nozzle blowing on them. The difference between the mixer and convergent nozzle test results reported in Ref. 12 and those reported here may be explained by the following considerations. The flap system used in the tests reported in Ref. 12 consisted of two flaps with leading and trailing edges. Thus, the leading as well as the trailing edge of each flap was exposed to the jet exhaust and both acted as noise sources. In the case of the configuration shown in Fig. 12, the trailing edge of the 43 cm long flat plate was located 5.08 centimeters beyond the nozzle axis; thus, in relation to the jet exhaust, the flat plate, effectively, did not have a leading edge. In addition to this difference, the mixer nozzle of Ref. 12 produced a decay in velocity at the flap to 63.5 percent of the nozzle exit velocity as compared to 45 percent produced by the 6-tube mixer nozzle, used here. Therefore, these distinctions may account for the difference in the noise reductions noted here and in Ref. 12.

Conclusions

The results of a preliminary experimental study of the effect on OASPL noise reduction produced by air blowing through a span-wise slot located near the trailing edge of a flat plate indicate that:

OASPL noise reductions no greater than 2.7 dB were obtained using the three test configurations with the slot located near the trailing edge of the plate and the plate positioned in the takeoff and landing configurations studied. And in the full scale configurations the PNL levels would probably produce less noise reduction. OASPL noise reductions of approximately 4 dB were obtained with the plate located 4 nozzle diameters downstream from the nozzle exit. By increasing the slot throat height by a factor of 2.4, an increase in noise reduction of 2 dB was found to be produced; reducing the lip length between the slot and trailing edge produced a negligible change in the reduction of noise.

With the slot located at the plate's trailing edge and the plate positioned to simulate the EBF landing configuration, results indicate that blowing through the 76 cm and 15 cm spanwise slots reduced the OASPL by the average values of 3.5 dB and 2 dB, respectively.

Of the five slot configurations studied, the following two produced the largest OASPL noise reductions in the landing EBF configuration; first, the 15 cm slot located at the flat plate's trailing edge, and second, the 15 cm slot located in a step near the trailing edge. At the same test position, these configurations produced similar OASPL noise reductions; however, spectral noise data show that the slot located at the plate's trailing edge may be more desirable. Specifically, the high frequency distribution above 2000 Hz was suppressed as much as 5.5 dB compared to 3.5 dB obtained using the step slot configuration. Moving the trailing edge to the jet axis, the spectral data show that the step slot configuration produces noise in the high frequency range above 2000 Hz at jet Mach numbers of 0.4 and 0.5, while a decrease in noise was produced using the configuration with the slot located at the plate's trailing edge.

A maximum difference in OASPL noise data of 14.5 dB was obtained between the jet exhaust issu-

ing from a 5.08 cm diameter convergent nozzle and a 6-tube mixer nozzle interacting with the trailing edge of a flat plate positioned in the EBF landing configuration. This difference was compared with a difference of 6 dB obtained from a similarly positioned large scale model of the EBF two flap configuration, a convergent nozzle, and a 7-lobe mixer nozzle. However, the flat plate studied here, effectively, did not have a leading edge. In addition, the 6-tube mixer nozzle, used here, produced a decay in velocity, at the flap, to 45 percent of its nozzle exit velocity compared to 63.5 percent for the 7-lobe mixer nozzle. Therefore, these dissimilarities may account for the differences in noise reductions.

Symbols

a	distance between the trailing edge of the plate and the axis of the convergent or mixer nozzle, has positive and negative values, see Fig. 2
D	convergent nozzle exit diameter
D_e	inside diameter of the mixer nozzle tubes
f	frequency
M_p	nozzle exit Mach number
M_{slot}	slot exit Mach number
v	nozzle exit velocity
x	distance from the trailing edge of the plate, measured parallel to its surface, to the downstream edge of the slot
y	slot height measured at its throat
z	axial distance between the exit plane of the nozzle, and its intersection with the plane of the plate
γ	acute angle between the plane of the plate and nozzle axis
θ	angle measured in the horizontal plane from the nozzle inlet along the microphone circle

References

1. Dorsch, R. G., Krejsa, E. A., and Olsen, W. A., "Blown Flap Noise Research," Paper 71-745, June 1971, AIAA, New York, N.Y.
2. Dorsch, R. G., Kreim, W. J., and Olsen, W. A., "Externally-Blown-Flap Noise," Paper 72-129, Jan. 1972, AIAA, New York, N.Y.
3. Goodykoontz, J. H., Dorsch, R. G., and Groesbeck, D. E., "Mixer Nozzle-Externally Blown Flap Noise Tests," TM X-68021, 1972, NASA, Cleveland, Ohio.
4. Olsen, W. A., Dorsch, R. G., and Miles, J. H., "Noise Produced by a Small Scale, Externally Blown Flap," TN D-6636, 1972, NASA, Cleveland, Ohio.
5. Olsen, W. A., Miles, J. H., and Dorsch, R. G., "The Noise Generated by the Impingement of a Jet Upon a Large Flat Board," TN D-7075, 1972, NASA, Cleveland, Ohio.
6. Hayden, R. E., "Noise from Interaction of Flow with Rigid Surfaces. A Review of Current Status of Prediction Techniques," NASA Contract NAS1-9599-14, BBN-2276, 1972, Bolt, Beranek and Newman, Cambridge, Massachusetts.
7. Pinkel, Benjamin, and Scharton, Terry D.: Reduction of Noise Generated by Flow of Fluid Over a Plate. Presented at the 84th Meeting of the Acoustical Society of America. Paper No. V - 5, Miami Beach, Florida, November 28, 1972.
8. Wagner, F. R., "The Sound and Flow Field of an Axially Symmetric Free Jet Upon Impact on a Wall," Zeitschrift für Flugwissenschaften, Vol. 19, no. 1, Jan. 1971, p. 30-44.
9. White, P. H., and Scharton, T. D., Simple Pressure Source Model of Jet Noise," Journal of the Acoustical Society of America, Vol. 51, no. 1, Pt. 1, Jan. 1972, p. 95.
10. von Glahn, U. H., Groesbeck, D. E., and Huff, R. G., "Peak Axial-Velocity Decay with Single- and Multi-Element Nozzles," Paper 72-48, Jan. 1972, AIAA, New York, N.Y.
11. Crow, S. C., and Champagne, F. H., "Orderly Structure in Jet Turbulence," Journal of Fluid Mechanics, Vol. 48, P. 3, Aug. 16, 1971, pp. 547-591.
12. Goodykoontz, Jack H., Dorsch, Robert G., and Groesbeck, Donald E.: Mixer Nozzle-Externally Blown Flap Noise Test. NASA TM X-68021, February 1972.

TABLE I. - SLOT CONFIGURATIONS AND SUBVARIATIONS

Slot configurations	Type of nozzle	z/D	a/D	γ , in degrees	x , cm	y/D	M_p	Slot length, cm	Type noise data taken
1(a)	convergent	4	-1,0,1	25	0.95	0.12	0.4,0.5,0.7,0.9	20	OASPL
1(b)	convergent	7	-1,0,1	60	0.95	0.12	↓	20	OASPL
1(c)	convergent	9	0,1,3,4	20	0.95	0.12		20	OASPL
2(a)	convergent	4	1	25	0.48,2.06	0.05	0.4,0.5,0.7,0.9	20	OASPL
2(b)	↓	7	0	60	2.06	0.05	↓	20	OASPL
2(c)		7	0,1	60	0.48	0.05		20	OASPL, SPL
2(d)		7	1	60	0.48,1.58,2.06	0.05		20	OASPL
2(e)		7	-1,0,1	60	1.58	0.05		20	OASPL, SPL
2(f)		9	-1,0,1,3,4	20	0.48	0.05		20	OASPL
3(a)	convergent	4	1	25	2.03	0.08	0.4,0.5,0.7,0.9	76	OASPL
3(b)	↓	7	1	60	2.03	0.1	↓	76	OASPL
3(c)		7	1,1.5	60	2.03	0.08,0.1		20	OASPL
3(d)		9	0	20	2.03	0.08		76	OASPL
4(a)	convergent	7	0,0.25	60	0	0.07,0.1	0.4,0.5,0.7,0.9	76	OASPL
4(b)	↓	7	-1,-3/8,0,0.5,1	60	0	0.05	↓	15	OASPL, SPL
4(c)		7	-1,0,0.5,1	60	0	0.1		20	OASPL
4(d)		9	0	20	0	0.1		76	OASPL
4(e)		9	0	20	0	0.12		20	OASPL
5(a)	convergent	7	0,0.5,1	60	0.64	0.05	0.4,0.5,0.7,0.9	15	OASPL, SPL
5(b)	convergent	7	0,0.5,1	60	1.19	0.05	0.4,0.5,0.7,0.9	15	OASPL, SPL
Slot configuration	Type of nozzle	z/D_e	a/D_e	γ , in degrees	x , cm	y/D_e	M_p	Slot length, cm	Type noise data taken
5(c)	mixer	16.1	0,2.3	60	1.2	0.12	0.4,0.5,0.7,0.9	15	OASPL, SPL

TABLE II. - OASPL NOISE REDUCTION IN DECIBELS WITHIN THE REGION
 $\theta = 90$ TO 135 DEGREES AT $z/D = 7$ AND $\gamma = 60$ DEGREES

M_p	Region of data at $a/D = 1$		Noise reduc- tion at $\theta = 90^\circ$	M_{slot}	x in cm	y/D	M_p	Region of data at $a/D = D$		Noise reduc- tion at $\theta = 90^\circ$	M_{slot}	x in cm	y/D
	lower limit in dB	upper limit in dB						lower limit in dB	upper limit in dB				
Slot Configuration 1; Slot Length = 20 cm													
0.4	-1	0	0	0.3	0.95	0.12	0.4	-1	-0.5	-0.8	0.28	0.95	0.12
0.5	-0.2	0.7	0.7	0.31			0.5	-1.5	-1	-1.25	0.33		
0.7	0	1.1	0.3	0.47	↓	↓	0.7	-1	-0.5	-1	0.45	↓	↓
0.9	0	1.9	0	0.48	↓	↓	0.9	-0.6	0	-0.6	0.52	↓	↓
Slot Configuration 2; Slot Length = 20 cm													
0.4	1.2	2.5	2.5	0.27	1.58	0.05	0.4	0	1.5	0	0.3	0.48	0.05
0.5	0	1	0.5	0.31	0.48		0.5	-0.9	1	-0.9	0.39		
0.7	0.2	1.5	0.35	0.39	0.48		0.7	-0.5	1.5	0.5	0.43		
0.9	0	2.7	0	0.33	0.48	↓	0.9	-2	1	1	0.68	↓	↓
Slot Configuration 3; Slot Length = 20 cm													
0.4	0	2	2	0.22	2.03	0.1							
0.5	1.25	1.25	1.25	0.31	↓								
0.7	0	1.2	0	0.43	↓								
0.9	0.5	2.5	0.5	0.6	↓	↓							

TABLE III. - OASPL NOISE REDUCTION IN DECIBELS WITHIN THE REGION
 $\theta = 90$ TO 135 DEGREES AT $z/D = 9$ AND $\gamma = 20$ DEGREES

M_p	Region of data at $a/D = 1$		Noise reduc- tion at $\theta = 90^\circ$	M_{slot}	x in cm	y/D	M_p	Region of data at $a/D = D$		Noise reduc- tion at $\theta = 90^\circ$	M_{slot}	x in cm	y/D
	lower limit in dB	upper limit in dB						lower limit in dB	upper limit in dB				
Slot Configuration 1; Slot Length = 20 cm													
0.4	0	1	0.7	0.24	0.95	0.12	0.4	0.5	2.7	2.7	0.25	0.95	0.12
0.5	-0.3	0.8	0.8	0.31	↓	↓	0.5	-0.9	0	0	0.28	↓	↓
0.7	0	1	1	0.36	↓	↓	0.7	-1	-0.2	-0.2	0.33	↓	↓
0.9	-0.6	0.8	0.8	0.4	↓	↓	0.9	-1.1	-0.2	-0.4	0.39	↓	↓
Slot Configuration 2; Slot Length = 20 cm													
0.4	0	1.4	1.4	0.25	0.48	0.05	0.4	0.6	1.7	1.7	0.22	0.48	0.05
0.5	-0.2	1	1	0.27	↓	↓	0.5	0	0.4	0.4	0.3	↓	↓
0.7	-0.7	1.3	0.5	0.33	↓	↓	0.7	0	1	0.5	0.31	↓	↓
0.9	-0.5	0.5	0.5	0.32	↓	↓	0.9	-1.1	0.2	0.2	0.38	↓	↓
Slot Configuration 3; Slot Length = 76 cm													
							0.4	0.2	1	1	0.24	2.03	0.08
							0.5	0.7	1	1	0.24	↓	↓
							0.7	-0.7	1	0.6	0.24	↓	↓
							0.9	0.5	-1	0.5	0.15	↓	↓

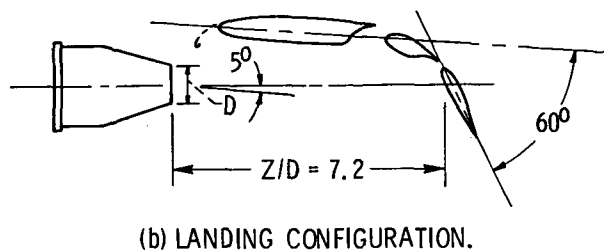
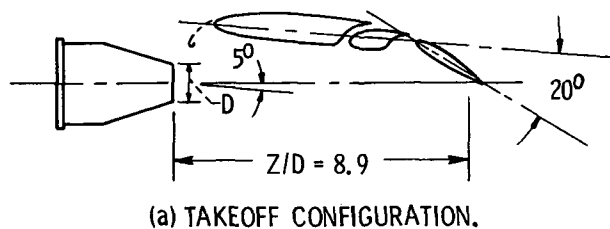


Figure 1. - Test configurations for externally blown flap model with convergent nozzle. Taken from reference 2.

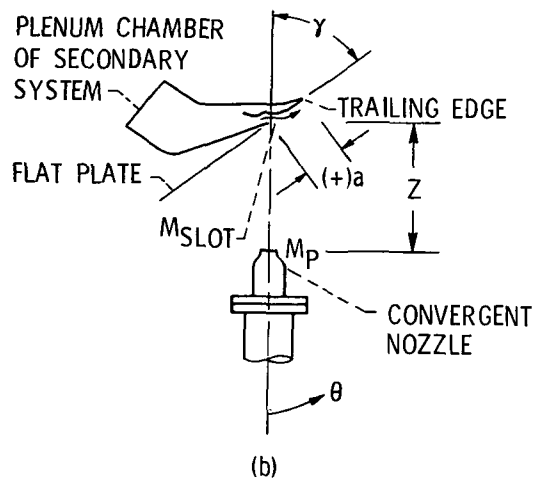
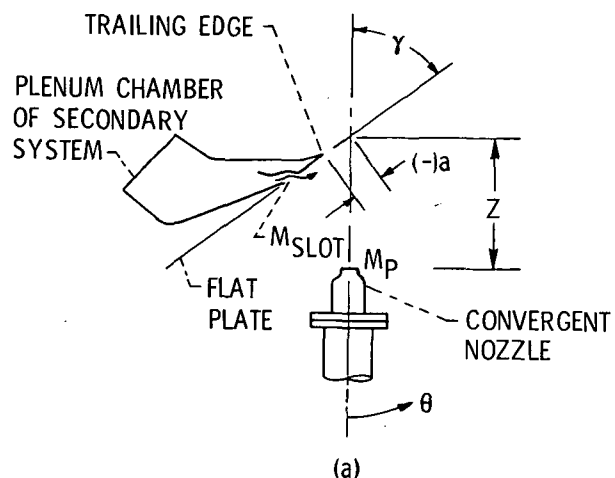
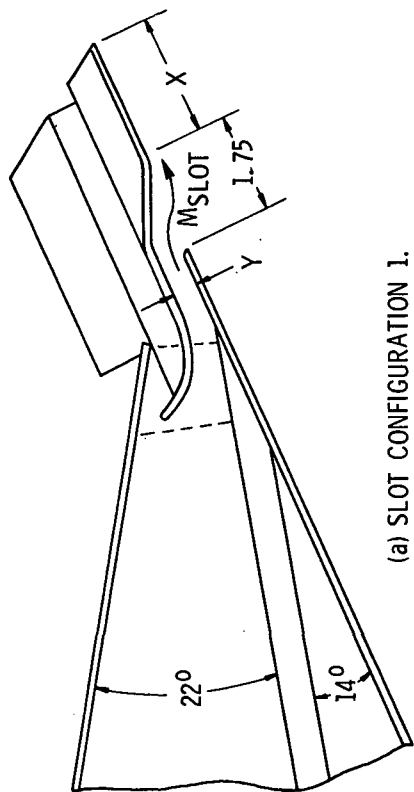
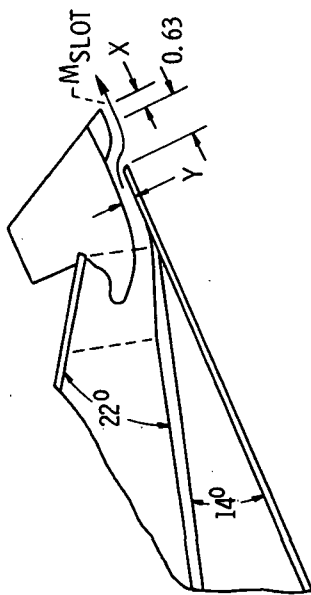


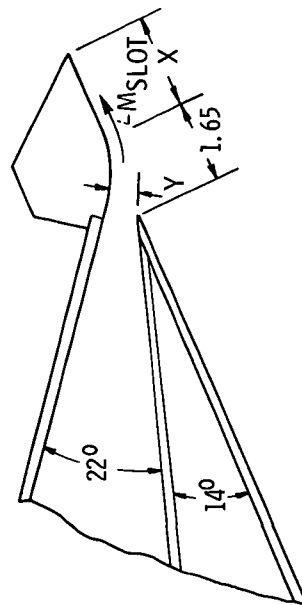
Figure 2. - Typical configuration with convergent nozzle and lateral movement of trailing edge ((+)a and (-)a).



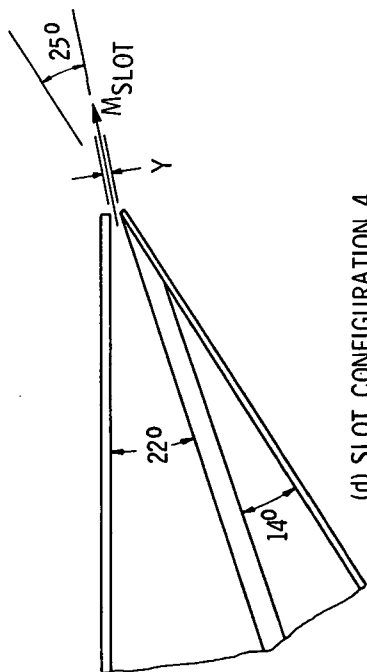
(a) SLOT CONFIGURATION 1.



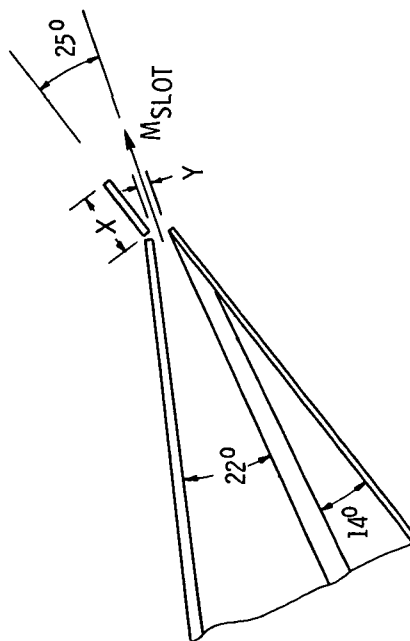
(b) SLOT CONFIGURATION 2.



(c) SLOT CONFIGURATION 3.



(d) SLOT CONFIGURATION 4.



(e) SLOT CONFIGURATION 5.

Figure 3. - Concluded.

Figure 3. - Sketches of slot configurations tested.

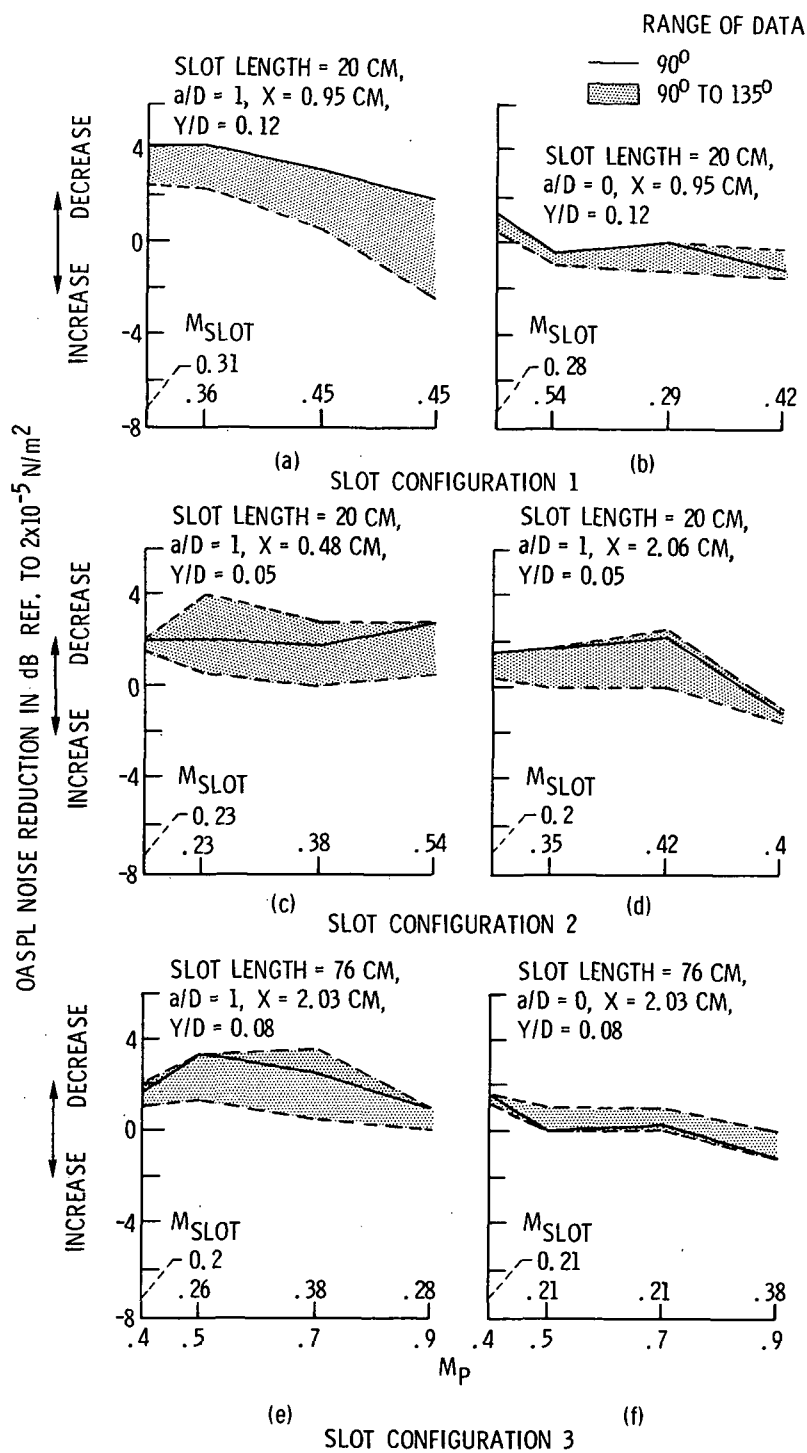


Figure 4. - OASPL noise reduction as a function of M_p for slot configurations 1, 2, and 3 at $Z/D = 4$ and $\gamma = 25^\circ$.

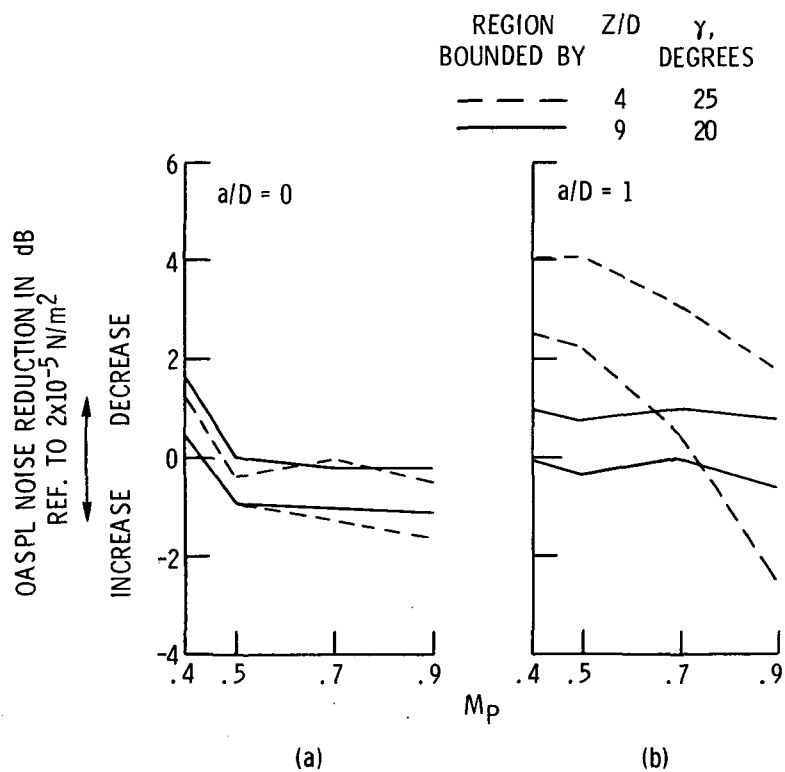


Figure 5. - Comparison of OASPL noise reduction as a function of M_p for slot configuration 1 showing the effect on noise reduction of a change in Z/D at a constant value of γ and a/D . $X = 0.95 \text{ cm}$ and slot length = 20 cm.

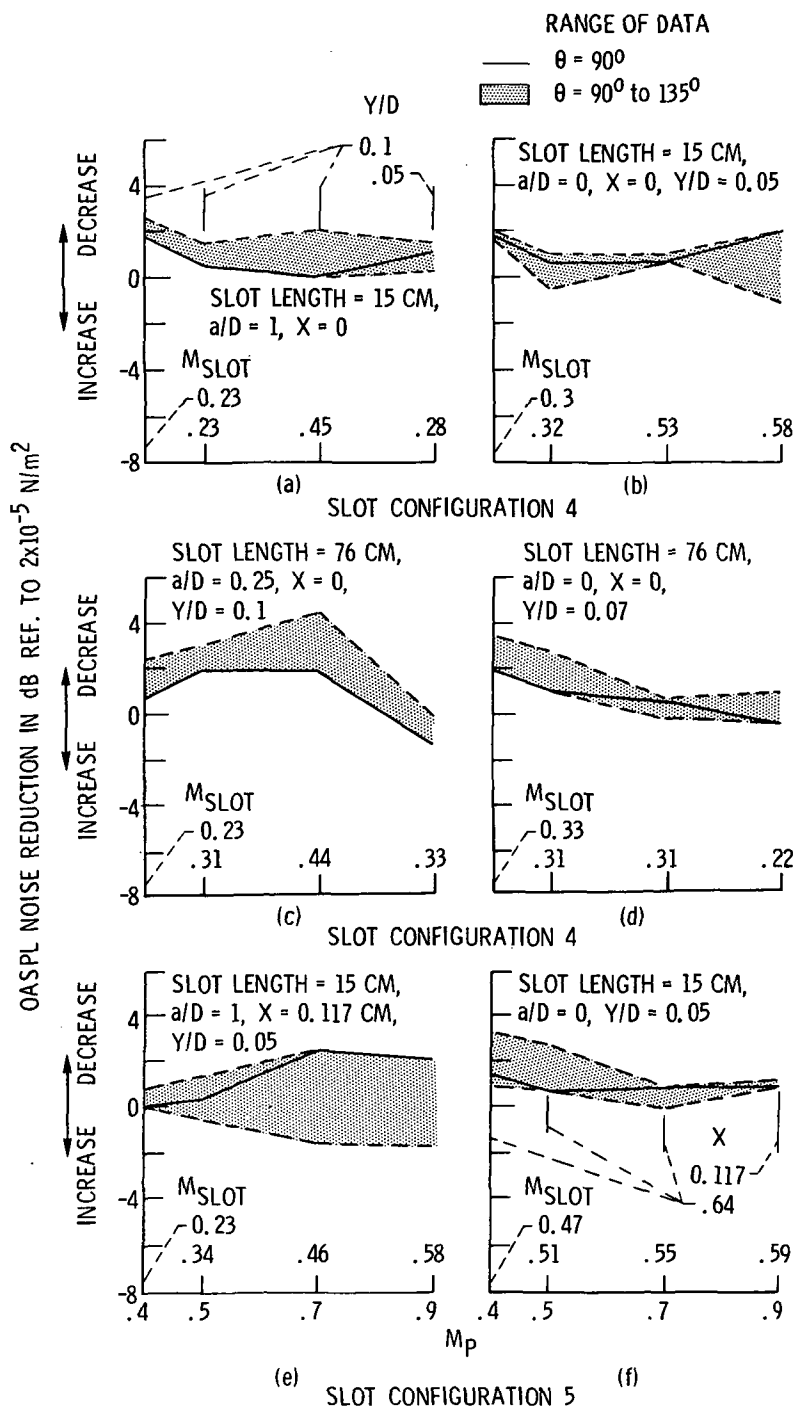


Figure 6. - OASPL noise reduction as a function of M_P for slot configurations 1, 2, and 3 at $Z/D = 7$ and $\gamma = 60^\circ$.

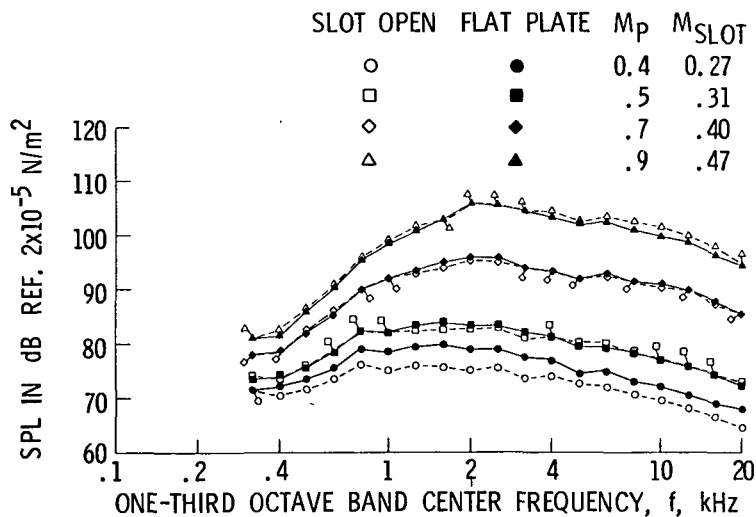


Figure 7. - One-third octave sound pressure level spectra showing a comparison between slot configuration 2 and flat plate data with jet exhaust impingement. $Z/D = 7$; $a/D = 1$; $\gamma = 60^\circ$; $X = 1.58$ cm; slot length = 20 cm; $\theta = 93^\circ$ on microphone circle.

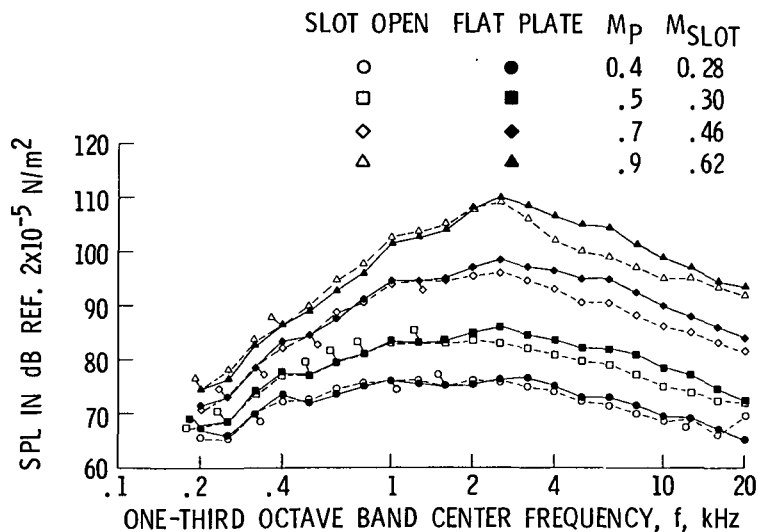


Figure 8. - One-third octave sound pressure level spectra showing a comparison between slot configuration 4 and flat plate data with jet exhaust impingement. $Z/D = 7$; $Y/D = 0.05$; $a/D = 1$; $\gamma = 60^\circ$; slot length = 15 cm; $\theta = 102^\circ$ on microphone circle.

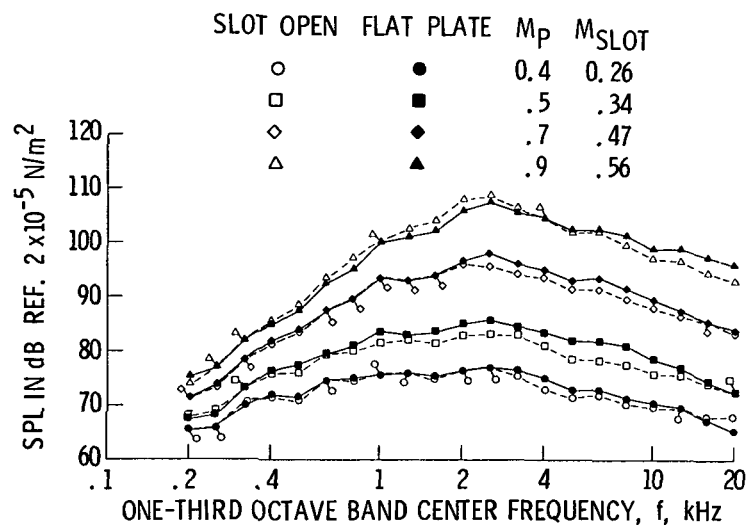


Figure 39. - One-third octave sound pressure level spectra showing a comparison between slot configuration 5 and flat plate data with jet exhaust impingement. $Z/D = 7$; $Y/D = 0.05$; $a/D = 1$; $\gamma = 60^\circ$; $X = 1.19$ cm; slot length = 15 cm; $\theta = 102^\circ$ on microphone circle.

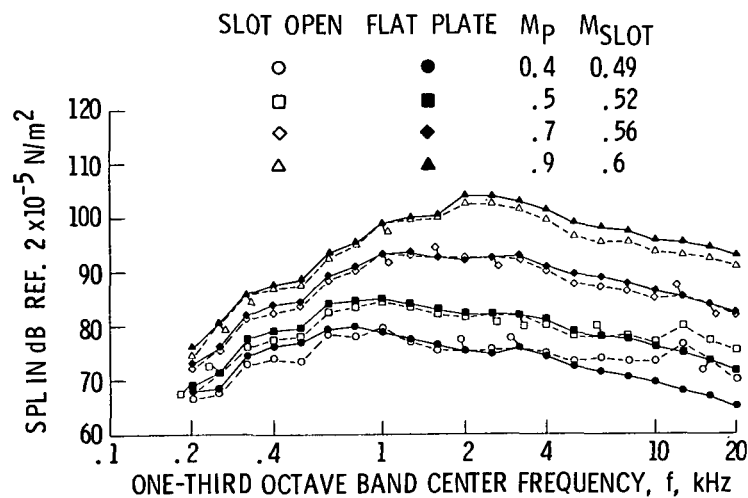


Figure 40. - One-third octave sound pressure level spectra showing a comparison between slot configuration 5 and flat plate data with jet exhaust impingement. $Z/D = 7$; $Y/D = 0.05$; $a/D = 0$; $\gamma = 60^\circ$; $X = 0.64$ cm; slot length = 15 cm; $\theta = 102^\circ$ on microphone circle.

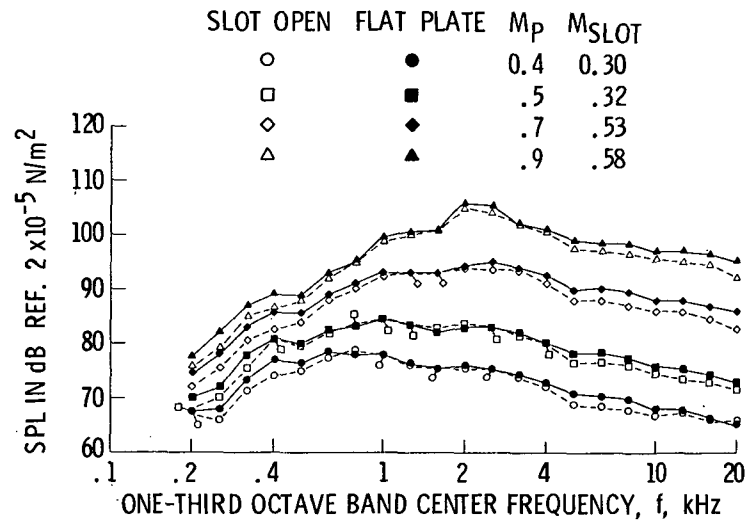


Figure 11. - One-third octave sound pressure level spectra showing a comparison between slot configuration 4 and flat plate data with jet exhaust impingement. $Z/D = 7$; $Y/D = 0.05$; $a/D = 0$; $\gamma = 60^\circ$; slot length = 15 cm; $\theta = 102^\circ$ on 3.05 m microphone circle.

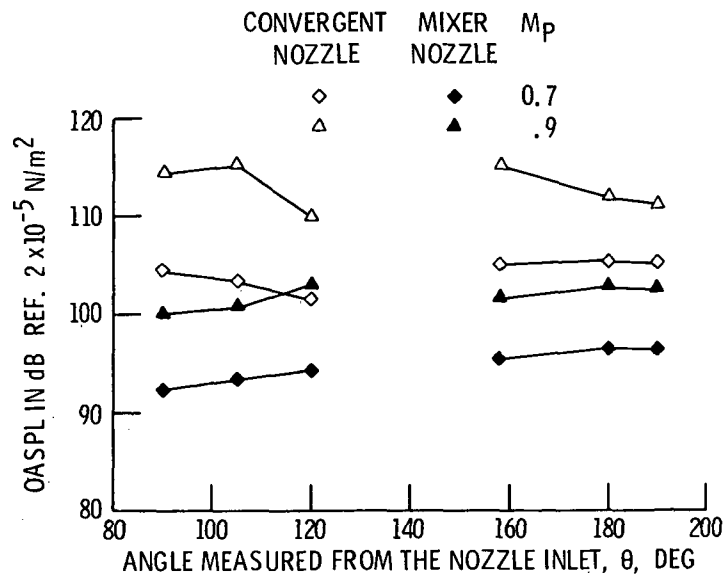


Figure 12. - Comparison between the sound field of a convergent nozzle and a 6-tube mixer nozzle with flow over the trailing edge of a flat plate in the EBF landing configuration. $\gamma = 60^\circ$; $a/De = 2.3$ and $Z/De = 16.1$.